Available online at www.sciencedirect.com
ScienceDirect
Earth and Planetary Science Letters 269 (2008) 131–139
EPSL
www.elsevier.com/locate/epsl

Energy partitioning during seismic slip in pseudotachylyte-bearing faults (Gole Larghe Fault, Adamello, Italy)

Lidia Pittarello [a], Giulio Di Toro [a,b,*], Andrea Bizzarri [c], Giorgio Pennacchioni [a,d], Jafar Hadizadeh [e], Massimo Cocco [d]

[a] *Dipartimento di Geoscienze, Università di Padova, via Giotto, 1, 35137-Padova, Italy*
[b] *Istituto di Geoscienze e Georisorse, Unità operativa di Padova, CNR, via Giotto, 1, 35137-Padova, Italy*
[c] *Istituto Nazionale di Geofisica Vulcanologia, Sezione di Bologna, via Donato Creti, 12, 40128–Bologna, Italy*
[d] *Istituto Nazionale di Geofisica Vulcanologia, Sezione di Roma, via di Vigna Murata, 605, 00143-Roma, Italy*
[e] *Department of Geography & Geosciences, University of Louisville, Louisville, Kentucky 40292, USA*

Received 4 June 2007; received in revised form 28 January 2008; accepted 30 January 2008
Available online 19 February 2008
Editor: R.D. van der Hilst

Abstract

The determination of the earthquake energy budget remains a challenging issue for Earth scientists, as understanding the partitioning of energy is a key towards the understanding the physics of earthquakes. Here we estimate the partition of the mechanical work density into heat and surface energy (energy required to create new fracture surface) during seismic slip on a location along a fault. Earthquake energy partitioning is determined from field and microstructural analyses of a fault segment decorated by pseudotachylyte (solidified friction-induced melt produced during seismic slip) exhumed from a depth of ~10 km—typical for earthquake hypocenters in the continental crust. Frictional heat per unit fault area estimated from the thickness of pseudotachylytes is ~27 MJ m^{-2}. Surface energy, estimated from microcrack density *inside* clast (i.e., cracked grains) entrapped in the pseudotachylyte and in the fault wall rock, ranges between 0.10 and 0.85 MJ m^{-2}. Our estimates for the studied fault segment suggest that ~97–99% of the energy was dissipated as heat during seismic slip. We conclude that at 10 km depth, less than 3% of the total mechanical work density is adsorbed as surface energy on the fault plane during earthquake rupture.

Keywords: earthquakes; pseudotachylyte; particle size distribution; energy partitioning; surface energy; frictional heat

1. Introduction

The earthquake energy balance states that the total (elastic and gravitational) energy variation is partly radiated out of the source and partly absorbed on the fault plane by fracturing and frictional dissipation (Kanamori and Rivera, 2006 and references therein). The energy adsorbed on the fault plane during seismic ruptures is the mechanical work E_f (Cocco et al., 2006, and references therein). In this study, we only consider the mechanical work density (work per unit area) since we are not interested here in the whole energy budget (which includes the radiated energy). At a specific point on the fault plane the mechanical work E_f is partitioned into heat (Q) and surface energy (U_s) (Kostrov and Das, 1988; Cocco et al., 2006):

$$E_f = Q + U_s \left[\mathrm{Jm}^{-2}\right]. \quad (1)$$

In general, Q includes frictional heat as well as the work done by other dissipative processes within the fault zone, such as high frequency stress waves radiated by crack tips and plastic deformation of grains (Kostrov and Das, 1988; Cocco et al., 2006). It is worth noting that the mechanical work partitioning defined in Eq. (1) cannot be estimated by seismological analyses, because it is impossible to evaluate the surface energy created during dynamic sliding from seismic waves. Moreover, seismological investigations can only provide an estimate of the

* Corresponding author. Dipartimento di Geoscienze, Università di Padova, via Giotto, 1, 35137-Padova, Italy. Tel.: +39 049 8271863; fax: +39 049 8272070.
E-mail address: giulio.ditoro@unipd.it (G. Di Toro).

0012-821X/$ - see front matter © 2008 Elsevier B.V. All rights reserved.
doi:10.1016/j.epsl.2008.01.052

breakdown stress drop from seismic waves, but the magnitude of the shear stress on a fault is unknown (unless under extremely favorable circumstances; see Spudich et al., 1998). Therefore, they cannot determine the total mechanical dissipation E_f during seismic slip (Kanamori and Heaton, 2000). For these reasons, we believe that the field and microstructural observations discussed in the present study provide a unique occasion to constrain the energy partitioning defined in Eq. (1).

Although some studies assume that fracture energy (G, the energy that controls the dynamics of a propagating rupture) represents the new surface created during slip (i.e., $G=U_s$, Yoshioka, 1986; Wilson et al., 2005), the fracture energy G should be not confused with the surface energy U_s. Indeed, several recent studies have shown that fracture energy contains an indefinite mixture of surface energy and heat (Tinti et al., 2005; Chester et al., 2005; Ma et al., 2006). G increases with earthquake size and it is of the order of 1–10 MJ m^{-2} for large earthquakes (Li, 1987; Tinti et al., 2005; Rice et al., 2005). However, the physical meaning of G and its contribution to the earthquake energy balance is still being debated within the scientific community (for an analysis on this issue, see Abercrombie et al., 2006: Earthquakes, Radiated Energy and the Physics of Faulting). Therefore, seismological investigations can provide an estimate of the fracture energy (or equivalently the breakdown work, as defined by Tinti et al., 2005), but they cannot evaluate its partitioning into surface energy and heat.

Here we attempt at using pseudotachylyte-bearing faults to get information on the energy partitioning between Q and U_s and to enlighten the physical meaning of G. Pseudotachylyte (solidified friction-induced melt produced during seismic slip) is the only fault rock univocally recognized as a record of an ancient seismic slip along an exhumed fault (Cowan, 1999). Unlike the case of pseudotachylyte-free faults (Chester et al., 2005; Keulen et al., 2007), it is possible to estimate Q from the volume of pseudotachylyte, without any assumptions regarding the frictional strength of the fault (Sibson, 1975; Di Toro et al., 2005a). In this framework, Q represents the work absorbed in frictional heating. In pseudotachylyte-bearing faults it is not easy to estimate the U_s associated with the seismic rupture, as the fine-grained fault rock precursory to, and simultaneous with, pseudotachylyte is consumed by the frictional melt. In fact comminution is often considered as an essential precursor to melting by friction (Spray, 1995). However, the pristine crushed rock may have locally escaped melting and be preserved *inside* some clasts (internally cracked grains, or fragmented grains where individual parts can be fit together, see Keulen et al., 2007) within pseudotachylyte, as it is the case investigated in this study. By comparing the surface energy estimated from the amount of new surface produced during seismic slip with the frictional heat estimated from pseudotachylyte vein thickness, we conclude that most mechanical work dissipated during an earthquake, at least at 10 km depth and in the studied fault segment, is heat.

2. Scientific rationale

Pseudotachylyte consists of a solidified melt including survivor clasts of the wall rock. For seismic melts, the frictional heat Q exchanged per unit fault area is (Di Toro et al., 2005a):

$$Q = \left[H(1-\phi) + c_p(T_m - T_{hr})\right] \rho\, w \quad \left[\mathrm{Jm^{-2}}\right] \tag{2}$$

where ϕ is the volume ratio between survivor clasts and the pseudotachylyte matrix, H is the latent heat of fusion, c_p is the specific heat at constant pressure, T_m is the maximum temperature achieved by the melt, T_{hr} is the host rock temperature, ρ is the rock density and w is the pseudotachylyte average thickness. Main assumption in Eq. (2) is that frictional heating is adiabatic at seismic slip rates (~1 m/s) and seismogenic depths (~10 km): the soundness of this assumption is confirmed by theoretical analysis (Di Toro et al., 2006). It follows that Q can be determined from field analysis by the measure of the pseudotachylyte *average thickness* (note that Q is an energy density).

The surface energy produced during rupture propagation is (Chester et al., 2005):

$$U_s = (A_{SZ} + A_{DZ})\gamma \quad \left[\mathrm{J\ m^{-2}}\right], \tag{3}$$

where A_{SZ} and A_{DZ} are the new surface per unit area produced in the slipping zone and in the damage zone of the wall rocks, respectively, and γ is the specific surface energy.

To determine the partitioning between surface energy and heat, we need to investigate fault segments exhumed from seismogenic depths that record a single seismic rupture that propagated trough an intact rock. Examples of these faults can be found in the Gole Larghe Fault in the Italian Southern Alps.

3. Selected pseudotachylyte-bearing fault segment within the Gole Larghe fault zone

The exhumed strike–slip Gole Larghe fault zone crosscut in an E–W-orientation the tonalites (granitoid rocks consisting of 48% plagioclase, 29% quartz, 17% biotite and 6% K-feldspar (Di Toro and Pennacchioni, 2005) of the Adamello batholith (Italian Alps). It is exposed in large (1 km × 0.5 km) and continuous glaciated outcrops allowing the structure of an exhumed seismogenic source to be investigated in detail (Di Toro and Pennacchioni, 2005). Deep creeks cutting the outcrop surface allow to reconstruct the 3D structure of the fault zone. The fault zone consists of ~200 main sub-parallel faults, exploiting a precursor set of joints, and was active ~30 Ma ago at 9–11 km depth and 250 °C host rock temperature (Di Toro and Pennacchioni, 2004; 2005; Pennacchioni et al., 2006). Fault rocks are cataclasites and pseudotachylytes, with the latter mostly developed during the last slip event along each fault. The cataclasites are cohesive fault rocks cemented by the widespread deposition of epidote, K-feldspar and minor chlorite due to fluid–rock interaction along the faults, mainly predating the production of pseudotachylyte (Di Toro and Pennacchioni, 2005). This type of epidote- and K-feldspar-bearing fault rocks are referred to as cataclasites in the following text. An ambient temperature of 250 °C during faulting is constrained by the development of the subgreenschist facies alteration (epidote + chlorite + titanite + plagioclase saussuritization) along faults, by the occurrence of local crystal plastic microstructures of quartz

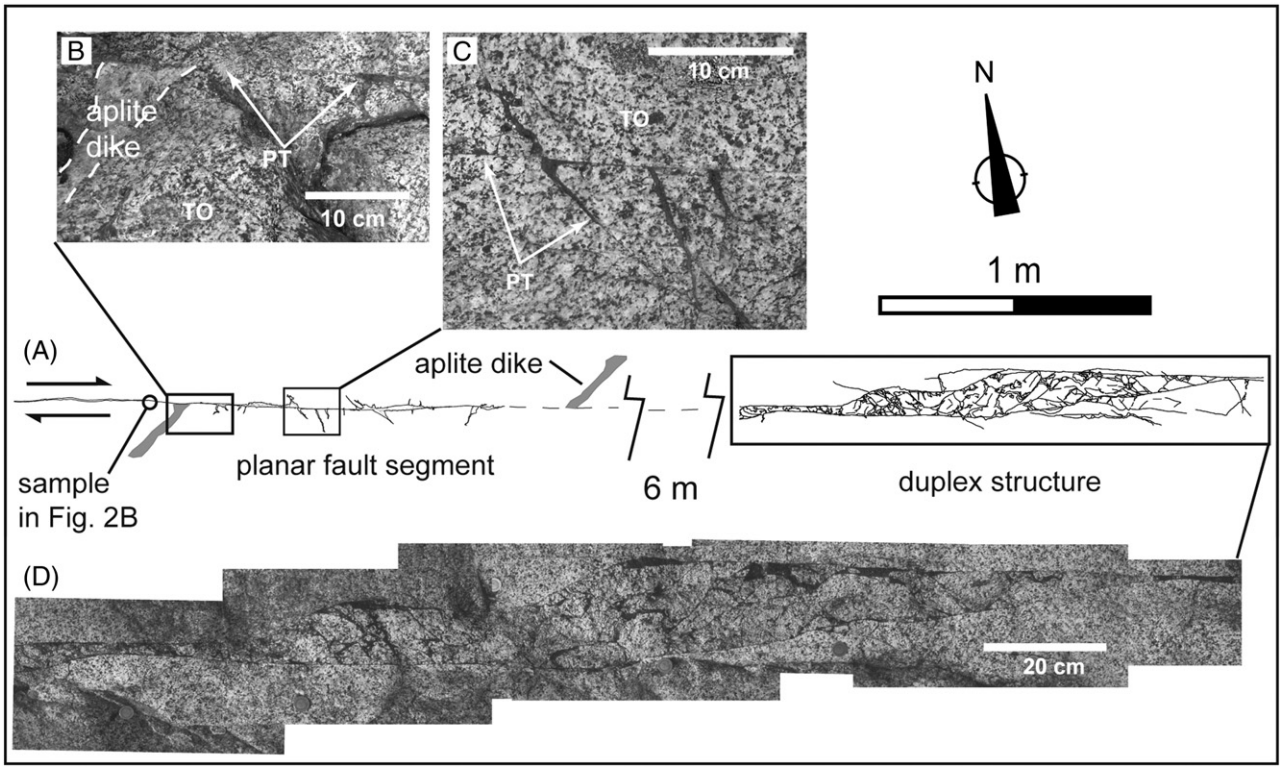

Fig. 1. The pseudotachylyte-bearing fault segment selected in this study. (A) The fault consists of a planar segment (to the left—also shown in Fig. 3A) and sinistral stepover (to the right) located six meters apart along the fault. (B) Along the planar fault segment an aplite dike shows a separation resulting from a coseismic slip of 1.44 m. (C) Detail of injection veins ramifying off the fault into the host rock. (D) Photomosaic of the breccia welded by pseudotachylyte developed at the left stepover of the fault. Note that the planar segment and the stepover are hosted in an non-altered host rock. Moreover, there are no clasts of altered host rock and cataclasite in the planar segment and in the pseudotachylyte breccia.

within some cataclasites, and by other geological constraints (Di Toro and Pennacchioni, 2004; 2005). A few fault segments contain only pseudotachylytes without a precursor cataclasite and, therefore, they record a single seismic slip event. The single-jerk nature of these fault segments is corroborated by several field (Fig. 1) and microstructural evidences (Fig. 2):

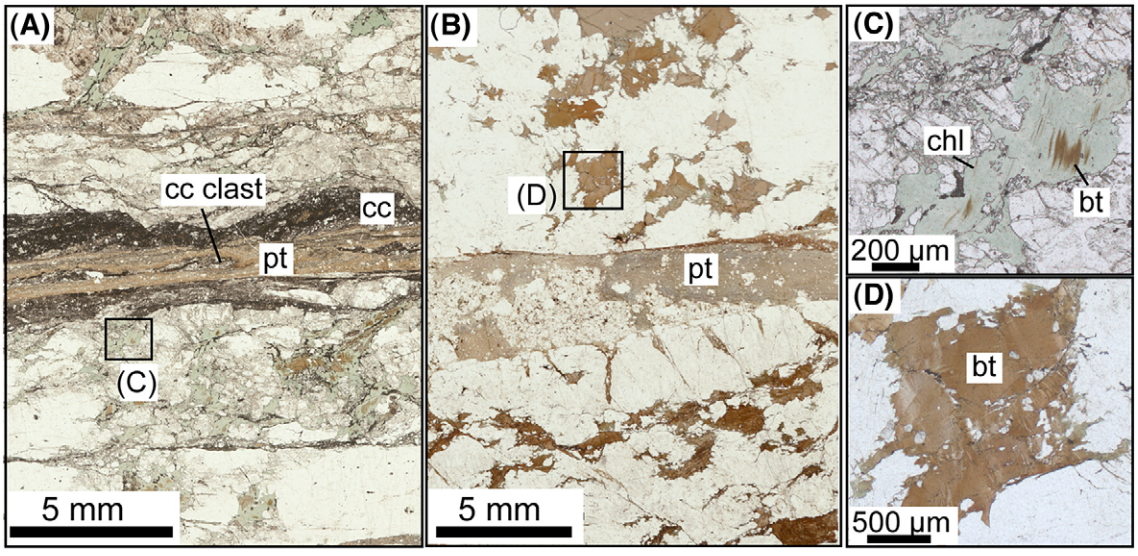

Fig. 2. Comparison between a fault with pseudotachylyte associated with precursor cataclasite and a fault with only pseudotachylyte. All pictures are optical microscope (polarized light) images. (A) Dark layers of cataclasite (cc) flank either sides of a pseudotachylyte vein (pt). The wall rock tonalite shows diffuse brittle deformation and a pervasive to complete alteration of the magmatic biotite (brown in color) to chlorite (green: inset C). The dusty gray zones of the tonalite are plagioclase altered to saussurite. (B) Pseudotachylyte vein within unaltered tonalite. The wall rock of the pseudotachylyte vein shows unaltered biotite (brown: inset D) and a "clean" plagioclase free of dusty alteration to saussurite. (C) Magmatic biotite (bt: brown in color) extensively pseudomorphosed into chlorite (chl: green) and titanite (dark grains) inside the altered tonalite. (D) Typical biotite in the fresh tonalite.

(1) the pseudotachylyte vein occur in contact with intact tonalite and it is not flanked by the cataclasite; (2) the host rock of the pseudotachylyte does not show the pervasive alteration of biotite (transformed to chlorite+titanite) and feldspar (saussuritized) which is instead typical of tonalite adjacent to cataclasite (Di Toro and Pennacchioni, 2005); (3) the pseudotachylyte does not contain clasts of cataclasite, which are common in pseudotachylyte associated with cataclasite, and (4) the pseudotachylyte form a single vein and there is no sign of multiple melting episodes; the zoning features of the vein are symmetric and referable to the cooling of the vein (chilled margin: Di Toro and Pennacchioni, 2004). The observations at points (2) and (3) apparently exclude that cataclasite was produced first and then it was completely consumed by frictional melting in the selected pseudotachylyte-bearing fault segments. One of these pseudotachylyte-bearing, cataclasite-free faults was selected for study and two separate portions of the faults (including a planar segment and a contractional stepover) are shown in Fig. 1. The planar fault segment crosscuts an aplite dyke and this allows the fault slip to be estimated. The seismic slip of 1.44 m can be estimated from the measured separation of the aplite dyke crosscut by the fault (Fig. 1). This amount of slip is roughly consistent with a M6–M7 earthquake (Sibson, 1989).

4. Field and microstructural data from the selected fault segment

The use of Eqs. (2) and (3) to estimate the energy budget partitioning from the exhumed fault requires the determination of both field and microstructural quantities from the pseudotachylyte-bearing fault. The average pseudotachylyte thickness w appearing in Eq. (2) is determined from field analysis. The new surface area ($A_{SZ}+A_{DZ}$) produced during seismic slip, used to estimate the U_s, is determined from microstructural analysis. Below it is explained how w and A_{SZ} were estimated in the selected fault segment, and why A_{DZ} can be assumed negligible. The parameters appearing in Eqs. (2) and (3), that are not a direct outcome of measurements of the current study, will be commented in the discussion section.

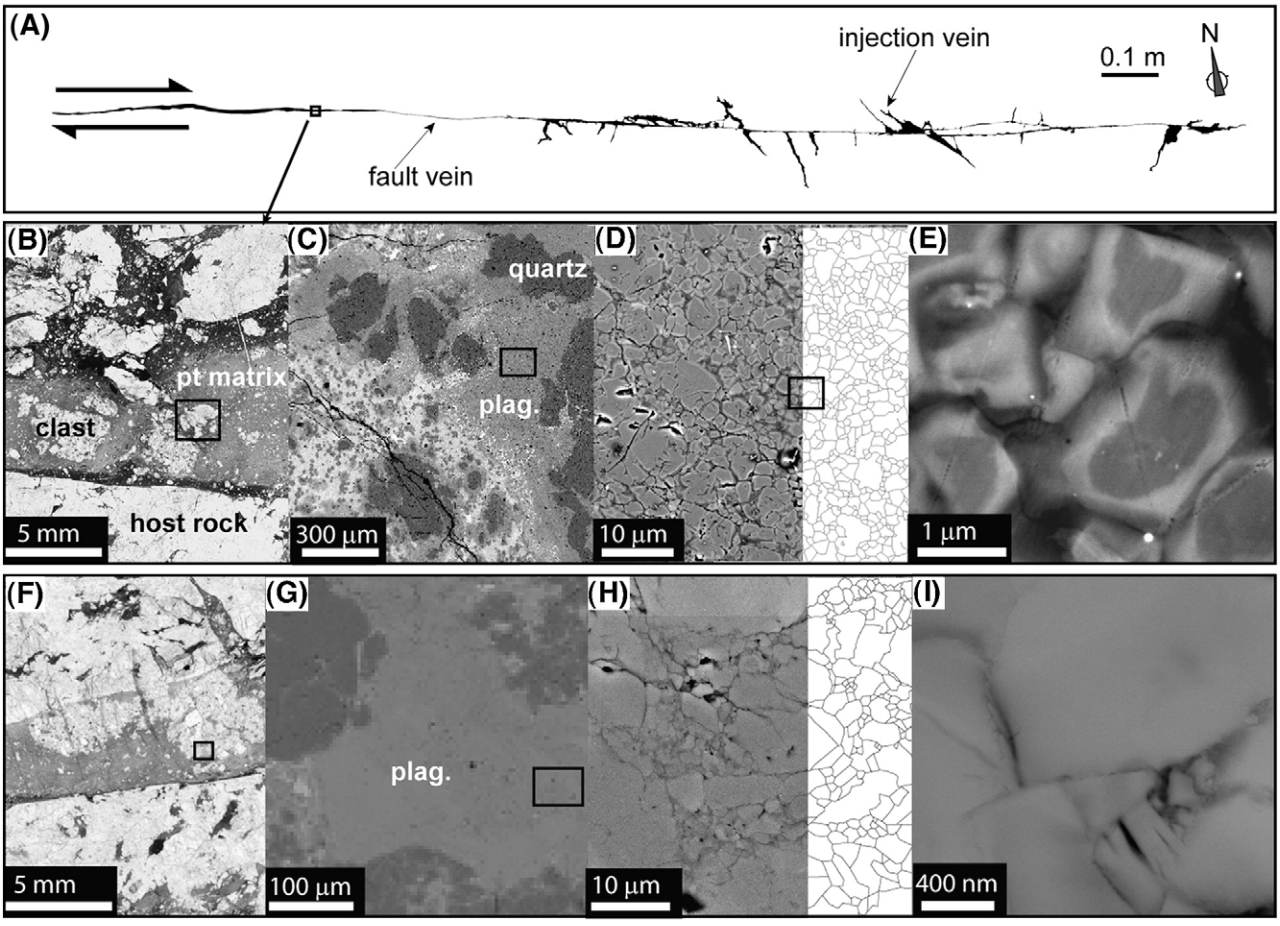

Fig. 3. Pseudotachylyte-bearing fault segment and microstructures in the pseudotachylyte. (A) Sketch of the pseudotachylyte-bearing fault segment selected for the estimate of frictional heat (see Fig. 1). The arrow indicates the location of samples used for the microstructural analyses. (B–E) Sequence of microphotos in a pseudotachylyte zooming in on type 1 (zoned) fragmented clasts. The boxes in the different photos show the location of the next photo on the left. The pseudotachylyte consists of clasts suspended in a glassy-like matrix (B: optical microscope, polarized light), consisting of quartz and plagioclase of a black and light gray color, respectively, in BSE SEM images (C). The plagioclase clasts show an internal fragmentation well evident in BSE SEM images (D). The network of fragment boundaries drawn from the photo is shown on the right of the photo. In the BSE FE-SEM image (E) the fragments are zoned with lighter Ca-enriched rims. (F–I) Sequence of microphotos (similar as in B–E) in a pseudotachylyte zooming in on type 2 fragmented clasts. Note that plagioclase fragments do not show any zoning under high magnification in the BSE FE-SEM image (I).

4.1. The average thickness of the pseudotachylyte vein

Pseudotachylyte vein networks are usually complex including both fault veins, along the slip surface, and injection veins ramifying off the fault into the host rock (e.g., Fig. 1B). Moreover, pseudotachylyte thickness may vary along strike due to the presence of pull apart and other surface irregularities. This is also the case of the pseudotachylytes from the fault segment selected in this study (Figs. 1 and 3A). The average vein thickness w appearing in Eq. (2) represents the thickness per unit fault length of the melt layer produced during seismic slip and includes the melt extruded from the slip surfaces into the injection veins. To estimate w we measured the outcrop surface area of pseudotachylyte from high-resolution digital photomosaics of the planar fault segment of Fig. 3A. The average thickness w is calculated as the ratio between the outcrop area of pseudotachylyte and the outcrop fault length according to the "area method" described in Di Toro et al. (2005a). This "average" pseudotachylyte thickness value was $w=5.9$ mm.

4.2. Fragment size distribution inside survivor clasts within pseudotachylyte

In the following text, we distinguished between clasts (i.e., survivor lithic clasts suspended in the solidified melt) and fragments (or fractured domains inside the survivor clasts). The pseudotachylytes typically contain clasts of fragmented quartz and plagioclase that survived melting (Fig. 3). The fragment size distribution within plagioclase clast cores was determined by computer-aided image analysis of standard Secondary Electron Microscope (SEM, resolution 200 nm) and a Field Emission SEM (FE-SEM, resolution 5 nm) photos (Fig. 3C–E; 3G–I). We used plagioclase for estimating U_s because:

1) fragments within plagioclase clasts are easily distinguishable in Back Scatter (BSE) SEM images (Figs. 3D, H);
2) plagioclase is the most abundant component of the tonalite (i.e., the plagioclase fragmentation is expected to contribute for the largest part to U_s value in the slipping zone);
3) the specific surface energy γ of plagioclase ($\gamma=10$ J m^{-2}) is one order of magnitude larger than the γ of quartz ($\gamma=1$ J m^{-2}x) (Bruce and Walsh, 1962).

Because plagioclase has an higher γ than quartz, considering plagioclase fragmentation as representative of whole coseismic fragmentation in the slipping zone results in an overestimate of the surface energy. As shown later, even under this (and others) conservative assumption U_s is largely subordinate to Q.

In FE-SEM images, fragments of plagioclase *inside* some clasts show a compositional zoning with the rim richer in Ca than the core (type 1 fragments, Fig. 3E). In these cases, it is locally evident a coalescence between neighbor small fragments (Fig. 3E). Inside other clasts, plagioclase fragments are not zoned (type 2 fragments, Fig. 3I).

We collected BSE FE-SEM images of different plagioclase clasts using a large range of magnifications (from 500× to 16,000×) (e.g., Fig. 3D–E, 3H–I). These images were used to measure the area A_f of the fragments. The fragment grainsize is expressed as the radius r of the area-equivalent circular particle (i.e., $r=(A_f/\pi)^{0.5}$). The smallest fragment observed in type 2 clasts has $r\sim25$ nm, well above the 5 nm resolution limit of the FE-SEM. The fragment size normalized distribution for all the collected images is reported in the log—log plot of Fig. 4A.

Each fragment size distribution is well approximated by a polyline consisting of different segments of slope D_i^* for distinct size intervals (e.g., Fig. 4B). For each of these size intervals, the distribution is power law:

$$N(r) = r^{-D_i^*}. \quad (4)$$

Following the common practice, we will refer to the fragment size distribution as "fractal", also in the case when the power law covers less than two decades (Malcai et al., 1997). In each fragmented clast, the "fractal dimension" D_i decreases with decreasing grains size from $2<D_i<4$ (for fragment sizes of $1<r<10$ μm) to $0.2<D_i<1$ (for fragment sizes of $0.02<r<1$ μm).

4.3. Fracturing in the wall rocks

At the outcrop scale, only a few fractures extend off the main fault (Fig. 1, see also Fig. 4 in Di Toro and Pennacchioni, 2005) suggesting that the contribution of large fractures to the surface area produced during seismic slip was negligible. At the microscopic scale the wall tonalite adjacent the pseudotachylyte fault vein show a network of micro-fractures (Fig. 5A). The density of these fractures (total fracture length over the area of the

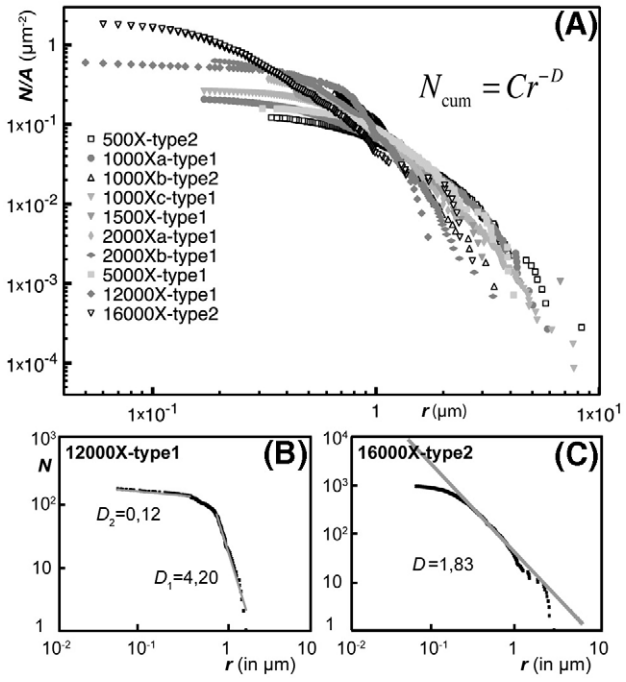

Fig. 4. (A) Normalized fragment size distributions inside the plagioclase clasts plotting the cumulative number of grains per total area of fragments versus the fragment radius. Gray and black symbols represent type 1 (zoned) and type 2 (non-zoned) fragments, respectively. (B) Representative type 1 fragment size distribution. (C) Representative type 2 fragment size distribution.

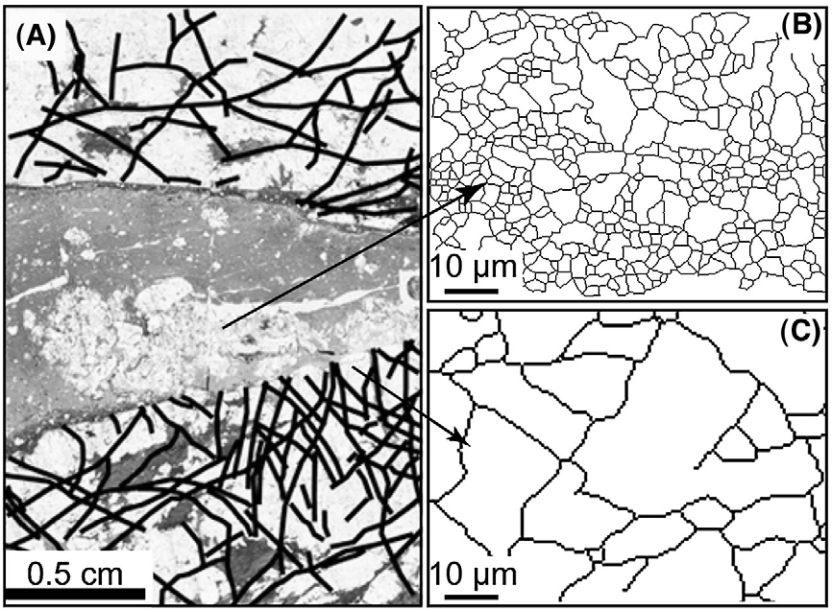

Fig. 5. Comparison between microfracture density within the clast inside the pseudotachylyte and in the adjacent wall rock damage zone. (A) Main network of microfractures (thick black lines) in the wall rocks of the pseudotachylyte drawn over an optical microscope photo at relatively low magnification (plane polarized light). (B) and (C) show, for a comparison, the network of microfractures (drawn from BSE SEM images of identical magnification) within plagioclase clasts inside the pseudotachylyte and in the wall rock, respectively.

image) at a distance <1 cm from the fault is ~300 times lower than in the clasts within the pseudotachylytes slipping zone (compare Fig. 5B with Fig. 5C). The microfracture density in the damage zone of a fault dramatically decreases away from the slipping zone (Wilson et al., 2003). We conclude that the new surface area generated in the fault wall rock is negligible compared to the new surface produced in the slipping zone.

5. Discussion

5.1. Estimate of the frictional heat

The determination of Q by Eq. (2) requires the estimate of seven parameters (w, ϕ, H, c_p, T_m, T_{hr} and ρ). In Section 4.1, the pseudotachylyte average thickness (w) was estimated to be 5.9 mm. The volume ratio between survivor clasts and the pseudotachylyte matrix (ϕ) of 0.2 was determined for the selected fault segment by Di Toro and Pennacchioni (2004). Based on the mean mineral composition of the microlitic matrix of the pseudotachylyte (80% plagioclase and 20% biotite) and on the estimated ϕ =0.2, the latent heat of fusion H results 3.32 10^5 J kg^{-1} (Di Toro and Pennacchioni, 2004). The specific heat at constant pressure c_p is ~1200 J $kg^{-1}K^{-1}$ (Di Toro and Pennacchioni, 2004). The tonalite density ρ is 2700 kg m^{-3} (Philpotts, 1990). The host rock temperature T_{hr} during seismic slip was ~250 °C, as indicated by several geological constraints, microstructural observations and petrographic data discussed in detail by Di Toro and Pennacchioni (2004). Assumed that textural zoning observed in thick (>6 mm) pseudotachylytes of the Gole Larghe fault resulted from differential cooling rates at the centre and periphery of the veins, Di Toro and Pennacchioni (2004) suggested a maximum temperature of the pseudotachylyte melt T_m of ~1450 °C based on numerical modeling of vein cooling. A T_m>1200 °C is also consistent with the clear evidence of melting of plagioclase clasts within pseudotachylytes. Therefore, the pseudotachylyte melt was superheated, which means that the melt temperature was higher than the equilibrium melting temperature and of the melting point of some rock-forming minerals (e.g., plagioclase). Superheating is explained by fast fusion (Fialko and Khazan, 2005) or viscous shear heating of the frictional melt (Nielsen et al., 2008). In this study we assume T_m=1450 °C. This temperature is in the range of the melt temperatures measured during high-velocity friction experiments in granitoid rocks (Spray, 2005).

Based on the above values of the Eq. (2) yields Q~27 MJ m^{-2}. This estimate of Q is comparable to that (8 MJ m^{-2}) based on electron spin resonance measurement of partial defect annealing in quartz found in the Nojima fault gouge and attributed to the M7.2 1995 Kobe earthquake (Matsumoto et al., 2001).

5.2. Estimate of the surface energy

Both the field investigation and the microstructural analysis indicate that the pseudotachylytes of the studied fault segment were not preceded by precursor cataclasites which, in contrast, commonly predate pseudotachylytes in most of the Gole Larghe faults (see Section 3). Therefore, the fragmentation observed *inside* clasts (i.e., internally cracked grains, Keulen et al., 2007) in pseudotachylytes has necessarily developed during the coseismic fracture propagation and slip, precursory (or synkinematic) of frictional melting. This fragmentation may result from processes such as abrasive wear (Rabinowicz, 1965), thermal fracturing (Ohtomo and Shimamoto, 1994) and process zone microfracturing (Reches and Dewers, 2005). The fragment distribution within clasts may be used to estimate the surface energy U_s provided no modification had occurred (e.g., by melting or growth) during the

high temperature stages of the seismic slip. This is probably true for type 2 fragments, which are not zoned.

The size distributions of both type 1 and type 2 fragments show a kink at about $r=1$ μm which is also observed in clast size distributions of feldspar within experimental cracked grains produced in granitoid rocks at 300 °C and in the absence of frictional melting (Heilbronner and Keulen, 2006; Keulen et al., 2007). This kink is probably related to a change in the deformation mechanism from brittle to plastic deformation at a critical grain size (r_{crit}) as demonstrated by Kendall (1978). According to the equation by Kendall (1978):

$$r_{crit} = \frac{16\ E\ \gamma}{3\ Y^2} \tag{5}$$

where E is the Young modulus (80 GPa), γ is the specific surface energy and Y is the yield strength (2.17 GPa) the calculated critical grain size is 0.9 μm (values for plagioclase with anorthite composition, Bass 1995). This value corresponds to the grain size at which the kink occurs in the studied fragment size distribution.

The above distribution is different from those observed in natural (Shimamoto and Nagahama, 1992) and experimental (Tsutsumi, 1999) pseudotachylytes that show a change in slope at larger clast sizes (5–10 μm) and have been interpreted to result from preferential melting of the finest particles (Shimamoto and Nagahama, 1992). The kinking of the fragment size distribution for grain sizes is (i) similar to that measured (~1 μm) in cracked grains in the absence of frictional melting and (ii) smaller than that measured (~5–10 μm) in the presence of melting. This suggests that the studied distributions were not strongly affected by melting.

Kinking in the distribution is more marked for type 1 than for type 2 fragments, with D_i values ranging from larger than 3 (for $r \geq 1$ μm) to less than 1 (for $r<1$ μm) (e.g., Fig. 4B). These D_i values are anomalous for standard fragmentation processes giving rise typically to two-dimensional D in the range of 1–2 (Sammis et al., 1986; Sammis and King, 2007). The presence of zoning and coalescence of type 1 fragments suggests that the type 1 fragment distribution may have been modified by growth, which likely occurred during the high temperature stages of cooling of the frictional melt embedding the clasts. The anorthite-rich composition and average thickness (~0.4 μm) of the rims of type 1 fragments is consistent with growth under superheated conditions of the friction-induced melt. The growth of these narrow rims has a strong effect on the size distribution. The number of finer fragments (<1 μm) decreases because of coalescence and results in the relatively low values (D_i~0.12 in Fig. 4B) (Sammis and Ben-Zion, in press). Instead, coalescence has the effect of increasing the number of fragments of grain size around 1 μm. The effect of the growth of the submicron-thick rims becomes more and more negligible with increasing fragment size (>1 μm). As a result, there is an increase in the D_i value (e.g. D_i=4.20, in Fig. 4B) in the size range of 1–10 μm.

The fragments of some plagioclase clast cores do not show any evidence of zoning or melting (type 2 fragments) and, therefore, they were probably not affected during the high temperature stages of the frictional process. The fragments size distribution in type 2 clasts is well approximated by a power law distribution with D_i~1.8 (Fig. 4C) for most of the fragment size range, except for the coarsest and finest fragments. This geometry of the distribution curve at the two extreme ends of distribution depends on an implicit limit of the grain size analysis method that leads to underestimate both the largest and smaller fragments. To correct the measured fragment size distribution from this artifact we have considered the size distribution as fractal, with a D~1.8 (typical for most of the grain sizes determined in this study) extended over the full range of observed fragment dimensions: 0.025–10 μm. This assumption, disregarding the grinding limit of the distribution, is conservative in the sense that by overestimating the number of the finest particles, it results in an overestimate of the total surface area and surface energy.

The corrected fragment distribution within type 2 clast may be assumed to represent the relict pristine microstructure produced during seismic fracture propagation and slip and is used to estimate U_s over the whole volume of pseudotachylyte. To estimate the total surface energy from measured fragment size distribution the 2-dimensional D of the distribution curve must be converted to the 3-dimensional D_{3D}according to the equation (Bonnet et al., 2001):

$$D^* = D + D' \tag{6}$$

where D' is a real number in the range (0,1). It follows that D^* is in a range of 1.83–2.83.

The total surface area of the fragments in the image area ($A^{image}{}_{SZi}$) can be calculated from the distribution curve as the integral:

$$A^{image}_{SZi} = \int_{r_{(min)}}^{r_{i(max)}} 4\pi\ r^2\ dN \approx \frac{4\pi\ CD_i^*}{2-D_i^*}\left(r_{i(max)}^{2-D_i^*} - r_{i(min)}^{2-D_i^*}\right) \tag{7}$$

where the $r_{i(max)}$ and $r_{i(min)}$ are the lower and upper size of the fragments (0.025 μm and 8.32 μm respectively) and C (33.69) is the ordinate axis-intercept of the straight line approximating the distribution. The resulting $A^{image}{}_{SZi}$ is in the range 4.08 10^3–3.02 10^4 μm^2.

To determine A_{SZ} (total surface of the fragments in the slipping zone for unit fault area), we determined how many times n the volume $V^{image}{}_{SZi}$ of the fragments (assumed as spherical) is included in the slipping zone V_{SZ} (in the studied fault segment, $V_{SZ}=w\cdot 1\ m^2=5.9\ 10^{-3}\ m^3$). From the fragment distribution (Eq. (4)):

$$V^{image}_{SZi} = \int_{r_{i(min)}}^{r_{i(max)}} \frac{4}{3}\pi r^3\ dN \approx \frac{4\pi\ C\ D_i^*}{3(3-D_i^*)}\left(r_{i(max)}^{3-D_i^*} - r_{i(min)}^{3-D_i^*}\right) \tag{8}$$

and

$$n = \frac{V_{SZ}}{V^{image}_{SZi}} \tag{9}$$

For the considered distribution and given the D^* values estimated above the equations yield $V^{image}{}_{SZi}$ in the range of 2.64 10^3–2.11 10^3 μm^3 and n=2.24 10^{12}–2.80 10^{12}.

The specific surface energy γ for plagioclase is 10 J m^{-2} (Bruce and Walsh, 1962). According to Eq. (3), the surface energy

in the slipping zone U_{s_SZ} can be estimated in the range of 0.10–0.85 MJ m^{-2}. As discussed in Section 4.3, the contribution in the new surface area from fractures in the host rock is negligible compared to fragmentation measured in the slipping zone and U_{s_SZ} can be taken as a good approximation of the total surface energy dissipated during seismic slip along the studied fault segment located at 10 km depth.

6. Conclusions

The above estimates indicate that the surface energy 0.10–0.85 MJ m^{-2} was negligible compared to Q (~27 MJ m^{-2}), and, from Eq. (1), $E_f \approx Q$ and $U_s/Q \approx 0.004$ to 0.03. It follows that, in silica-built rocks and at the nucleation depth (~10 km) of the earthquake analyzed here, the surface energy was less than 3% of the total mechanical work E_f and most of the energy absorbed on the fault was dissipated as frictional heat. However, in the case of seismic ruptures propagating at very shallow depths (<2 km, the Bosman Fault, South Africa, Reches and Dewers, 2005; the Mojave section of the San Andreas Fault, Dor et al., 2006) the amount of surface energy could be larger.

The small values for U_s/Q are consistent with those determined in low-velocity friction experiments ($U_s/Q < 0.1\%$, Yoshioka, 1986) and in industrial milling and grinding processes ($U_s/Q < 1\%$, Harris, 1966).

How does U_s relates to the seismological determined fracture energy G? Di Toro et al. (2005b) found $G > 8$ MJ m^{-2} to sustain rupture propagation in the case of the fault segment shown in Fig. 1. Therefore, our estimates indicate that U_s is negligible compared to G. These estimates corroborate the interpretation that most of fracture energy is actually dissipated as heat. For this reason Tinti et al. (2005) and Cocco et al. (2006) defined the fracture energy as breakdown work, being the only portion of E_f that is measurable through seismological analyses. However, we point out that the estimates determined in the present study arise from field observations and microstructural studies and not from theoretical predictions.

There is another original contribution in the present study. The surface energy U_s is estimated for a single seismic rupture (i.e., a single earthquake) and the inferred value is consistent with the mean of U_s values estimated for an *a priori* assumed number of seismic ruptures in exhumed strands of the San Andreas Fault system (Chester et al., 2005). In other words, the main advantage of using pseudotachylytes to infer the energy partitioning during an earthquake is that it allows the absolute values of both Q and U_s to be estimated independently and for a single seismic rupture. We believe that the energies estimated in the present study are useful for the understanding of the earthquake energy balance, at least at earthquake nucleation depths of about 10 km, and they provide a reliable measure of the order of magnitude of the whole mechanical work absorbed during earthquake ruptures.

Acknowledgments

F. Mulargia, S. Nielsen, Z. Reches, P. Spudich and E. Tinti are thanked for discussions. An anonymous reviewer is thanked for his constructive comments. INGV, JEOL and ZEISS are thanked for collecting FE-SEM images. A. Novello and L. Tauro are thanked for sample preparation. The costs of this study were covered by grants from the Università degli Studi di Padova (Progetto di Ateneo 2003), INGV 2006, MUR 2006–2007 and CARIPARO. J. Hadizadeh was supported by NSF-Earth 0229654 during the course of this study. Image analysis was conducted with SXM Image.

References

Abercrombie, R., McGarr, A., Di Toro, G., Kanamori, H., 2006. Earthquakes: Radiated Energy and the Physics of Faulting, Geophysical Monograph Series, vol. 170. American Geophysical Union, Washington, D.C. ISBN: 978-0-87590-435-1, pp. 1–327.

Bass, J.D., 1995. Elasticity of minerals, glasses and melts. In: Ahrens, T. (Ed.), A Handbook of Physical Constants. Mineral Physics and Crystallography, AGU Reference Shelf 2, Washington D.C., pp. 45–63.

Bonnet, E., Bour, O., Odling, N.E., Davy, P., Main, I., Cowie, P., Berkowitz, B., 2001. Scaling of fracture systems in geological media. Rev. Geophys. 39, 347–383.

Bruce, W.F., Walsh, J.B., 1962. Some direct measurements of the surface energy of quartz and orthoclase. Am. Mineral. 47, 1111–1122.

Chester, J.S., Chester, F.M., Kronenberg, A.K., 2005. Fracture surface energy of the Punchbowl Fault, San Andreas System. Nature 437, 133–136.

Cocco, M., Spudich, P., Tinti, E., 2006. On the mechanical work absorbed on faults during earthquake ruptures. In: Abercrombie, R.E., Mc Garr, A., Kanamori, H., Di Toro, G. (Eds.), Radiated Energy and the Physics of Earthquake Faulting, AGU Monograph Series 170, Washington D.C., pp. 237–254.

Cowan, D.S., 1999. Do faults preserve a record of seismic faulting? A field geologist's opinion. J. Struct. Geol. 21, 995–1001.

Di Toro, G., Pennacchioni, G., 2004. Superheated friction-induced melts in zoned pseudotachylytes within the Adamello tonalites (Italian Southern Alps). J. Struct. Geol. 26, 1783–1801.

Di Toro, G., Pennacchioni, G., 2005. Fault plane processes and mesoscopic structure of a strong-type seismogenic fault in tonalites (Adamello batholith, Southern Alps). Tectonophysics 402, 54–79.

Di Toro, G., Hirose, T., Nielsen, S., Shimamoto, T., 2006. Relating high-velocity rock friction experiments to coseismic slip in the presence of melts. In: Abercrombie, R., McGarr, A., Kanamori, H., Di Toro, G. (Eds.), Radiated Energy and the Physics of Faulting, Geophysical Monograph Series, vol. 170. American Geophysical Union, Washington, D.C., pp. 121–134.

Di Toro, G., Pennacchioni, G., Teza, G., 2005a. Can pseudotachylytes be used to infer earthquake source parameters? An example of limitations in the study of exhumed faults. Tectonophysics 402, 3–20.

Di Toro, G., Nielsen, S., Pennacchioni, G., 2005b. Earthquake dynamics frozen in exhumed ancient faults. Nature 436, 1009–1012.

Dor, O., Ben-Zion, Y., Rockwell, T.K., Brune, J., 2006. Pulverized Rocks in the Mojave section of the San Andreas Fault Zone. Earth Planet. Sci. Lett. 245, 642–654. doi:10.1016/j.epsl.2006.03.034, 2006.

Fialko, Y., Khazan, Y., 2005. Fusion by earthquake fault friction: stick or slip? J. Geophys. Res. 110. doi:10.1029/2005JB003869.

Harris, C.C., 1966. On the role of energy in comminution: a review of physical and mathematical principles. Trans. Inst. Min. Metall. C 75 C37–C56.

Heilbronner, R., Keulen, N., 2006. Grain size and grain shape analysis of fault rocks. Tectonophysics 427, 199–216.

Kanamori, H., Heaton, T.H., 2000. Microscopic and macroscopic physics of earthqukes. In: Rundle, J., Turcotte, D.L., Klein, W. (Eds.), GeoComplexity and the Physics of Earthquakes, AGU Monograph Series 120, Washington D.C., pp. 147–163.

Kanamori, H., Rivera, L., 2006. Energy Partitioning During an Earthquake, AGU Monograph Series 170, Washington D.C., pp. 3–14.

Kendall, K., 1978. The impossibility of comminuting small particles by compression. Nature 272, 710–711.

Keulen, N., Heilbronner, R., Stünitz, H., Boullier, A.-M., Ito, H., 2007. Grain size distributions of fault rocks: a comparison between experimentally and naturally deformed granitoids. J. Struct. Geol. doi:10.1016/j.jsg.2007.04.003..

Kostrov, B., Das, S., 1988. Principles of Earthquake Source Mechanics. Cambridge University Press, London.

Li, V.C., 1987. Mechanics of shear rupture applied to earthquake zones. In: Atkinson, B.K. (Ed.), Fracture Mechanics of Rocks 2nd edn. Academic, London, pp. 351–428.

Ma, K.F., Song, S.R., Tanaka, H., Wang, C.Y., Hung, J.H., Tsai, Y.B., Mori, J., Song, Y.F., Yeh, E.C., Sone, H., Kuo, L.W., Wu, H.Y., 2006. Slip zone and energetics of a large earthquake from the Taiwan Chelungpu-fault Drilling Project (TCDP). Nature 444, 473–476.

Malcai, O., Lidar, D.A., Biham, O., Avnir, D., 1997. Scaling range and cutoffs in empirical fractals. Phys. Rev. E 56, 2817–2828.

Matsumoto, H., Yamanaka, C., Ikeya, M., 2001. ESR analysis of the Nojima fault gouge, Japan, from the DPRI 500 m borehole. Isl Arc 10, 479–485.

Nielsen, S., Di Toro, G., Hirose, T., Shimamoto, T., 2008. Frictional Melt and Seismic Slip. J. Geophys. Res. 113. doi:10.1029/2007JB005122 B01308.

Ohtomo, Y., Shimamoto, T., 1994. Significance of thermal fracturing in the generation of fault gouge during rapid fault motion: an experimental verification (in Japanese with English abstract). Struct. Geol. 39, 35–44.

Pennacchioni, G., Di Toro, G., Brack, P., Menegon, L., Villa, I.M., 2006. Brittle–ductile–brittle deformation during cooling of tonalite (Adamello, Southern Italian Alps). Tectonophysics 427, 171–197.

Philpotts, A.R., 1990. Principles of Igneous and Metamorphic Petrology. Prentice Hall, Englewood Cliffs, New Jersey.

Rabinowicz, E., 1965. Friction and Wear of Materials. John Wiley, New York.

Reches, Z., Dewers, T.A., 2005. Gouge formation by dynamic pulverization during earthquake rupture. Earth Planet. Sci. Lett. 235, 361–374.

Rice, J.R., Sammis, C.G., Parsons, R., 2005. Off-fault secondary failure induced by a dynamic slip–pulse. Bull. Seismol. Soc. Am. 95, 109–134.

Sammis, C.G., King, G.C.P., 2007. Mechanical origin of power law scaling in fault zone rock. Geophys. Res. Lett. 34. doi:10.1029/2006GL028548 L04312.

Sammis, C.G., Ben-Zion, Y., in press. Mechanics of grain-size reduction in fault zones. J. Geophys. Res. 113. doi:10.1029/2006JB004892.

Sammis, C.G., Osborne, R.H., Anderson, J.L., Banerdt, M., White, P., 1986. Self-similar cataclasis in the formation of fault gouge. Pure Appl. Geophys. 124, 53–78.

Shimamoto, T., Nagahama, H., 1992. An argument against the crush origin of pseudotachylytes based on the analysis of clast size distribution. J. Struct. Geol. 14, 999–1006.

Sibson, R.H., 1975. Generation of pseudotachylyte by ancient seismic faulting. Geophys. J. R. Astron. Soc. 43, 775–794.

Sibson, R.H., 1989. Earthquake faulting as a structural process. J. Struct. Geol. 11, 1–14.

Spray, J.G., 1995. Pseudotachylyte controversy: fact or friction? Geology 23, 1119–1122.

Spray, J.G., 2005. Evidence for melt lubrication during large earthquakes. Geophys. Res. Lett. 32. doi:10.1029/2004GL022293.

Spudich, P., Guatteri, M., Otsuki, K., Minagawa, J., 1998. Use of fault striations and dislocations models to infer tectonic shear stress during the 1995 Hyogo-ken (Kobe) earthquake. Bull. Seism. Soc. Am. 88, 413–427.

Tinti, E., Spudich, P., Cocco, M., 2005. Earthquake fracture energy inferred from kinematic rupture models on extended faults. J. Geophys. Res. 110. doi:10.1029/2005JB003644 B12303.

Tsutsumi, A., 1999. Size distribution of clasts in experimentally produced pseudotachylyte. J. Struct. Geol. 21, 305–312.

Wilson, J.E., Chester, J.S., Chester, F.M., 2003. Microfracture analysis of fault growth and wear processes, Punchbowl Fault, San Andreas system, California. J. Struct. Geol. 25, 1855–1873.

Wilson, B., Dewers, T., Reches, Z., Brune, J., 2005. Particle size and energetics of gouge from earthquake rupture zones. Nature 434, 749–752.

Yoshioka, N., 1986. Fracture energy and the variation of gouge and surface roughness during frictional sliding of rocks. J. Phys. Earth 34, 335–355.